Non-Uniformly Distributed-Turns Coil Antenna for Enhanced H-Field in HF-RFID

Ashwani Sharma, Ignacio J. Garcia Zuazola, *Member, IEEE*, Anshu Gupta, Asier Perallos, *Member, IEEE*, and John C. Batchelor, *Senior Member, IEEE*

***Abstract*—A design study of coil antennas aimed to be used as Interrogators in high-frequency (HF) radio frequency identification (RFID) is presented. The magnetic field (H-field) of the coil is enhanced by defining optimally the number of turns of the antenna, and optimizing and exploiting the internal area of an initial coil. The distributed turns coil antennas are designed for highest possible H-field without compromising the Q-factor of the antenna with respect to an initial design. To achieve best solution, a non-uniformly distributed turns design is proposed and whose radiating elements are formulated accordingly. The analytical and simulated results show reasonable agreement to validate the designs. The enhanced H-field of the antenna shows an unconstrained Q-factor, indicates a potential rise to the interrogating coverage and as a result a higher efficient antenna.**

***Index Terms*—Coupling coefficient, H-field, inductance, magnetically coupled coils, quality factor, radio frequency.**

I. Introduction

THE need for automation and advanced technology in applications like tracking, packaging, transportation, and sensing has attracted the interest in using emerging radio frequency identification (RFID) technology. In RFID, radiated power is propagated and the information that is contained in the propagated envelope communicated wirelessly between a interrogator (sometimes called reader) and a transponder (Tag). The two way communication and information transfer is feasible only when both devices (Interrogator and Passive Tag) are tuned to a common shared frequency of operation. The choice of this operating frequency depends on several factors, e.g., application, propagation range, device dimension, and the surroundings. As far as the range is concerned, from the basics of antenna theory [1] we know that the field around an antenna can be divided in two regions: 1) near-field reactive (dominantly magnetic field (H-field)) and 2) far-field radiation (electromagnetic (EM) waves). The near-field RFID systems employ inductive coupling between the Tag and the Interrogator [2]. The power is induced in the Tag antenna by a reactive H-field oscillating near to the Interrogator antenna. The far-field RFID systems uses the real power of propagating EM waves for coupling the two devices [3]. The near-field RFID systems typically operate in the low frequency (LF) and high frequency (HF) bands. The prototype antennas at these frequencies are commonly electrically small (compared to wavelength) and have very low radiation resistance suitable for near-field reactive energy. In contrast, the far-field RFID systems operate at higher frequency e.g., ultra high frequency (UHF) and millimeter wave bands such that enough far-field radiation can be propagated by an antenna. The antennas operating at LF and HF are impractical for far field operations due to the physical size limitations.

For certain applications, which demand relatively low data rate (106 kbps [4]) and a small read out distance (< 1 m), the HF 13.56 MHz band is the preferred choice [5] because of two main reasons. First, since this band is internationally allocated for unlicensed use worldwide, the designed system has the possibility to perform anywhere in the world. Second, the magnetic field propagation at HF (HF-RFID) penetrates dielectric materials with high permittivity, such as water and the ground, better than the EM waves at UHF (UHF-RFID) in short range applications. Hence, HF-RFID is the preferred in very dense surroundings. In this paper, we focus on the designated central frequency 13.56 MHz inductively coupled HF-RFID systems using passive Tags. To accomplish a high performance operation, the HF-RFID systems need to be carefully designed.

Various studies are dedicated in the literature for RFID system architecture and design methodology. For instance, in [6], a RFID system architecture is presented where the transmit and receive (Tx/Rx) modules are conveniently designed using commercially available circuit blocks. In [7], the authors describe the circuit design of a transceiver and related data processing for RFID systems. In [8], the HF-RFID reader is developed using silicon phosphate (SiP) technology, and the authors in [9], analyze the HF-RFID and propose a system compatible with multiple standards. The contributions above [6]–[9] focus on the RFID module design, but do not consider the optimization of the antenna as an important notion to enhance the performance of the HF-RFID system. Since the radiated power and data transfer between the Interrogator and the Tag is materialized using antennas, the optimization of antennas is crucial to achieve best system performance and therefore a higher read range.

For low-cost RFID systems, coil antennas are widely used for both the Interrogator and the Tag [2], [10]–[13]. Because of the near-field mutual inductance at HF, both antenna coils act

Manuscript received April 08, 2013; accepted July 15, 2013. Date of publication July 30, 2013; date of current version October 02, 2013. This work was supported in part by the European Union through a Predoctoral Research Grant (FPI-Deusto 2011-2015).

A. Sharma, I. J. G. Zuazola, and A. Perallos are with the Deusto Institute of Technology—DeustoTech, University of Deusto, 48007 Bilbao, Spain (e-mail: ashwani.sharma@deusto.es; i.j.garcia@deusto.es; perallos@deusto.es).

A. Gupta is with the Helmut Schmidt University, 22043 Hamburg, Germany (e-mail: gupta@hsu-hamburg.de).

J. C. Batchelor is with the Department of Engineering and Digital Arts, University of Kent, Canterbury, Kent CT2 7NT, U.K. (e-mail: J.C.Batchelor@kent.ac.uk).

Color versions of one or more of the figures in this paper are available online at http://ieeexplore.ieee.org.

Digital Object Identifier 10.1109/TAP.2013.2275244

as a loosely (roughly) magnetically coupled transformer, where energy is magnetically induced and propagated from source to destination. Therefore, unlike far-field antennas which are characterized by gain, directivity, and radiation pattern, the coil antennas in near-field are best characterized by the following parameters; the coupling coefficient (k) between the Interrogator and the Tag coils, H-field (H) at the receiving Tag coil, inductance L of the coils, and unloaded quality Q factor of the antenna. In other words, the antenna coils are designed accordingly and with the following parameters optimized: the geometry and dimension (in radius) of the coils, the section of the wire (in radius), and the number of turns [14]. In the literature, a set of studies is dedicated to the design of RFID Tags for the read range increase [11]–[13] and antenna size reduction [15]–[17]. The Tag is designed for a low-cost, low profile, and electrically small solution [11]. In these designs, the Tag antenna coils capture H-field with a sufficient power to activate the Tag chip. Along with the Tag, the Interrogator coil should also be optimized for maximum power transfer (reactive energy).

Further work has been reported in [12], [18]–[20] where mutual coupling between the coil antennas is enhanced and the H-field given by an Interrogator antenna studied. Since the interrogation zone of a HF-RFID system is dependent on the antennas performance, the design of an Interrogator coil antenna for a predefined Tag is discussed in [18] and the optimum size of the coil formulated for a fixed reading range [5]. Once the coil antenna size is optimized, the internal area of the coil can be exploited [12] to enhance the H-field [20] For example, an increase in the number of turns (a multi-turn coil) and spacing between the resulting elements is an attractive approach to enhance the H-field of the Interrogator that is at a predefined distance of a Tag [12], [14], [20]–[22]. Yet, the H-field enhancement has been achieved solely when the Interrogator L was constant [19]; this however is at the expense of a 25% reduction in the Q-factor (increases the antenna loss and lowers its efficiency) according to [20]. This is because, the Interrogator coil resistance R increases with the number of turns, and if L is constant it will result in a lower quality, Q, [18], given by

$$Q = \frac{\omega \cdot L}{R}. \tag{1}$$

This approach is termed constant-L design. For highest energy transfer, Q should be high to minimize loss. In [19], a multi-turn coil is designed for an enhanced H-field without compromising Q.

In contrast, Q, which is inversely proportional to BW, is best to be low for demanding high data transfer. In [23], a design study of a RFID system is presented, which suggests that the Q of an Interrogator coil antenna should be as small as possible when reliable data transfer is aimed. This observation is followed in [18], [23], [24], where the authors proposed an Interrogator antenna coil having only one turn, single turn coil (STC) antenna, which in fact had the minimum achievable Q suitable for reliable data transmissions. In addition, the dimension of the coil was optimized for maximum H-field. Consequently, to enhance the H-field of the STC antenna with low Q, a similar approach is applied to exploit the internal area of the STC by adding several inward turns. Earlier, the constant-L approach seemed inappropriate for H-field enhancement due to the detuning of a targeted Q value. Although, the H-field enhancement approach presented in [19] for unconstrained Q seems appropriate, later it will be unfortunately seen as an impractical solution. Therefore, an optimized design with enhanced H-field and comparable Q performance to that of a STC antenna is necessary to investigate. In this paper, the aim is to optimally design a new antenna coil prototype for an improved transmission link-budget in HF-RFID systems.

To enhance the H-field of the Interrogator, the internal area of the coil antenna is parametrically studied to find optimal turn radii of the coil. For the approach, we assumed an initial design (optimal STC antenna according to [18], [23]) with a Q equal to that of a final proposed design Distributed-Turns Coil antenna (DTC), all presented in Fig. 2. The initial STC is depicted in Fig. 2(a) and has an optimal outer radius a_0 as proposed in [18]. In our study, we optimally design a DTC antenna which has an identical (or very close) Q as the STC antenna but achieves a significantly enhanced H-field. A possible solution is a uniformly distributed-turns coil (UDTC), [12], [19], [20] shown in Fig. 2(b), which has an equal spacing Δ between the adjacent turns. We will show, however, that this approach is unattractive for providing an optimal solution in prospective designs. We propose instead, a novel approach that exploits the utilization of turns in a more efficient manner; this is, by allowing the turns to have unequal spacing between them and Fig. 2(c) shows our first time proposed non-uniformly distributed-turns coil (NDTC) antenna design. In essence, the distributed turns of the coil, given by a_N, results in an unconstrained Q as compared to that of the STC, and allows for an adjusted L without detuning its resonance (13.56 MHz). To maintain resonance, any variation in L is compensated by adjusting the lumped capacitance of a matching network of the Interrogator equivalent circuit [5]. Prominent results will show an eminent NDTC antenna design with an enhanced H-Field; this is an improvement up to 116.23% and unconstrained Q, compared to the initial STC design.

The rest of the paper is organized as follows. Section II models the HF-RFID system and the design of the Interrogator and the Tag coils is presented. The distributed-turns coil designs are described in Section II-C. Section III presents the proposed NDTC antenna and the analytical solution for the optimal design. The analytical and simulated results are presented in Section IV and the paper is concluded in Section V.

II. HF-RFID System Modeling and Design

The HF-RFID system is now modeled and designed. The concluding inductively coupled HF-RFID equivalent circuit model, including both, the Interrogator and the Tag is presented in Fig. 1. The Interrogator coil antenna is represented by coil inductance L_{Tx} and coil resistance R_{Tx}, where the latter represents the ohmic losses of the coil. The Interrogator coil antenna is fed with a current source I_s having an internal resistance R_s. To maximize the power transfer between the source and the Interrogator coil antenna and allow for highest resonance at the antenna, a matching network is intercalated between the source and the Interrogator coil antenna to match the antenna impedance to that of the source. An L-match circuit using

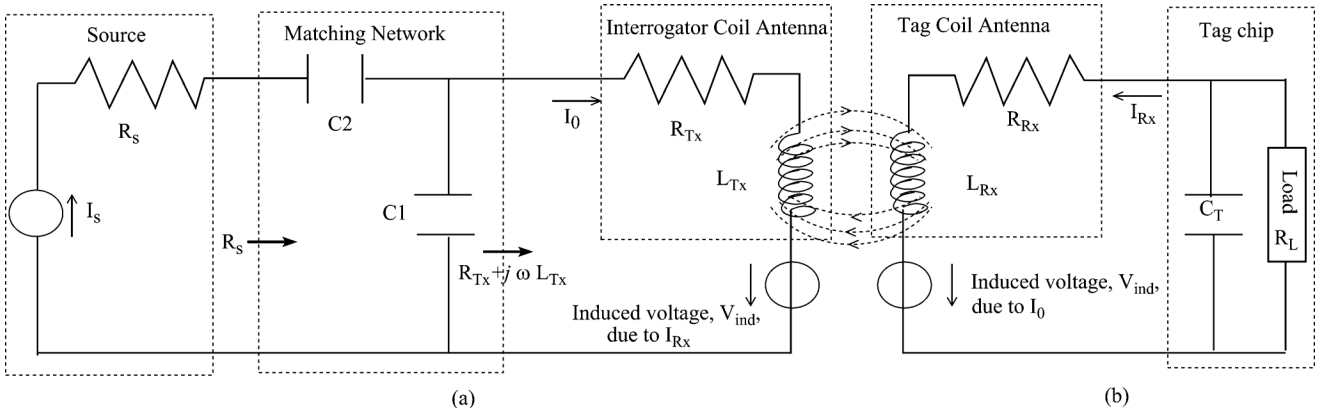

Fig. 1. Inductively coupled HF-RFID equivalent circuit model, (a) Interrogator and (b) Tag.

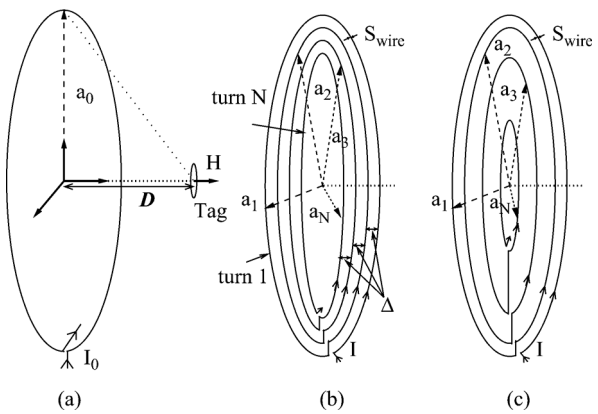

Fig. 2. Coil antennas: (a) single turn coil (STC), (b) uniformly distributed-turns coil (UDTC), (c) non-uniformly distributed-turns coil (NDTC).

lumped capacitances $C1$ and $C2$ forms the matching network; a simple and low-cost realization [5], [25] matches the antenna impedance to a standard $R_s = 50\Omega$.

Similarly, the Tag equivalent circuit is modeled and presented in Fig. 1(b), where the inductance and resistance of the Tag coil antenna are given by L_{Rx} and R_{Rx}, respectively. The Tag is powered (inductively coupled) by an induced voltage, V_{ind}, due to a current flow I_0 in the Interrogator coil antenna, Fig. 1(a). As a matter of fact, the resulted current, I_{Rx}, in the Tag coil, Fig. 1(b), backs an induced voltage in the Interrogator coil. The influence of the Tag on the Interrogator circuit has been studied in [26], and modeled in [23] via transformed Tag impedance (TTI), R_{TTI} (a measure of the performance, not a physical impedance the coil), and is simplified as

$$R_{TTI} = \omega k^2 L_{Tx} Q_{Rx} \tag{2}$$

where Q_{Rx} is the quality factor of the Tag and k is the coupling coefficient between the Interrogator and the Tag coils. Further rigorous study conducted in [26] demonstrated that it is necessary to maximize R_{TTI} for an optimized RFID system design. The maximum R_{TTI} response is achieved by maximizing Q_{Rx} (presented in Section II-A) and $k^2 L_{Tx}$ (presented in Section II-B).

A. Tag Coil Antenna

In this work, we use a pre-defined Tag coil from [23]; the equivalent circuit is presented in Fig. 1(b). In [23], maximum Q_{Rx} was targeted and BW was key to reliable data transmissions. The Tag was designed to receive efficiently the H-field induced by an Interrogator and made achievable by optimizing the Tag coil area A_{Rx} (antenna's physical aperture) and the total number of turns N_{Rx}. Our intention is to design solely the Interrogator coil antenna and enhance its reactive H-field with respect to the pre-defined Tag.

B. Interrogator Coil Antenna

The Interrogator coil antenna is now designed. Based on [12], [23] we will be showing how the coil design parameters are carefully selected to achieve an optimized performance. We assume a predefined interrogating distance D (read range). Because of the near-field coupling for inductive antennas, D is limited to $D \ll \lambda/2\pi \approx 4m$ (chap. 5 of [1]) for the operating central frequency $f = 13.56$ MHz. In this section, the theoretical analysis of an Interrogator coil design [8], [23] is reviewed and initially, we consider an electrically small circular coil [1] antenna with a current I_0 at its input port. Since the coil is electrically small, the current I_0 is assumed constant throughout the length of the wire, therefore, the H-field components that originate are in phase and positively contribute to the near-field propagation performance [18]. This initial antenna coil consists of N_0 number of turns whose windings are concentrated in close proximity to the outer winding (radius a_0). For this coil the optimum design parameters are evaluated meeting the following criteria.

1) a_0 , Dimension: Using the maximization of quantity, $k^2 L_{Tx}$, in (2), we subsequently show that $k^2 L_{Tx}$ is equivalent to H. From [21], we know that the induced voltage, V_{ind}, in a Tag is given by

$$V_{ind} = j2\pi f \cdot k \cdot \sqrt{L_{Tx} \cdot L_{Rx}} \cdot I_0 \tag{3}$$

and from Faraday's law, the following expression is known:

$$V_{ind} = \mu_0 \cdot j2\pi f \cdot N_{Rx} \cdot A_{Rx} \cdot H \tag{4}$$

where μ_0 is the free space permeability. Equating (3) with (4), we obtain the following relation:

$$k^2 L_{Tx} = \left(\frac{\mu_0 \cdot N_{Rx} \cdot A_{Rx}}{\sqrt{L_{Rx}}} \frac{H}{I_0} \right)^2. \tag{5}$$

Observation suggests that $k^2 L_{Tx}$ can be expressed solely as H/I_0 when a tag is predefined (N_{Rx}, A_{Rx}, L_{Rx}) ($\mu_0 \approx 1$). Therefore, for a given Tag, $R_{TTI}(2)$ can be simplified and be equal to $k^2 L_{Tx}(5)$ and therefore to H/I_0. Hence, the maximization of R_{TTI} is equivalent to the maximization of H/I_0 which according to [18] is related to N_0, a_0, and D and given as:

$$\frac{H}{I_0} = \frac{N_0 a_0^2}{2\left[\sqrt{(a_0^2 + D^2)}\right]^3}. \tag{6}$$

Because I_0 is assumed constant and D is predefined, H depends solely on the geometric properties (a_0 and N_0) of the Interrogator coil antenna. Using (6)H is maximized by appropriate selection of a_0 and N_0. The optimum a_0 is targeted for a maximized H at a predefined D, and is derived as a function of D[18] as $a_0 = \sqrt{2}D$ (for $D \leq 1$ m [26]) .

2) n_0, Number of Turns: Typically, the design of an Interrogator coil for a given Tag at a given D should be such that it provides the Tag with a sufficient H to activate the Tag chip [19]; that is, a minimum required H (H_{min}). N_0 is found using $I_0 \times N_0 = \sqrt{27} H_{min} D$ from [18]. Because I_0 and D are constant, N_0 is found in regards to H_{min}. However, a high N_0 is limited by the Q-factor of the Interrogator antenna $Q_0 = 2\pi f \cdot L_{Tx}/R_{Tx}$ which is inversely proportional to the BW of the antenna [23], [27]; that is, as N_0 increases, Q_0 also increases, and the BW reduces. Hence, N_0 is chosen such that Q does not rise above a desired value. For reliable data transmissions, authors in [18], [23] proposed $N_0 = 1$ to achieve the lowest Q_0 possible.

Using the immediately described criteria we introduce an optimum Interrogator coil antenna [18], [23] with $a_0 = \sqrt{2}D$, $N_0 = 1$, corresponding inductance L_0, resistance R_0, and the restricted $Q_0 = 2\pi f \cdot L_0/R_0$. The resulted design is named an STC antenna and shown in Fig. 2(a). To impedance match the STC antenna to the Interrogator source, $C1$ and $C2$, Fig. 1(a), are chosen so that the coil can resonate at $f = 13.56$ MHz.

We note from (6) that, to further improve the H of the STC antenna N_0 should be increased above 1. But, an increment of N_0 (becomes a multi-turn coil) causes unacceptable reduction in BW due to the increased Q. Hence, a design whose method can enhance H while maintaining Q equal to that of the STC antenna, Q_0, is needed. We showed in [19], that the use of finite spacing Δ between two adjacent turns is an attractive approach to improve H without compromising Q. We hereby propose Distributed-Turns coil antennas in Sections II-C and III, that overcomes previous works on coil designs by enhancing H without compromising Q.

C. Distributed-Turns Coil Design

A derivative of a DTC antenna is now presented. A typical DTC is expressed by a radius vector $\mathbf{A} = [a_1, a_2, \ldots a_N]$ and a_i is the radius of i^{th} turn, Fig. 2. The DTC designs have a number of turns $N > 1$, hence, appropriate to improve H over the STC antenna, Section II-B. In this section, the claim is demonstrated and corroborated by a skilled analysis and fair comparison of a number of DTC antennas. The analysis aptitude is mainly given by N and the spacing between the turns possible for an improved H coil antenna with an unconstrained Q.

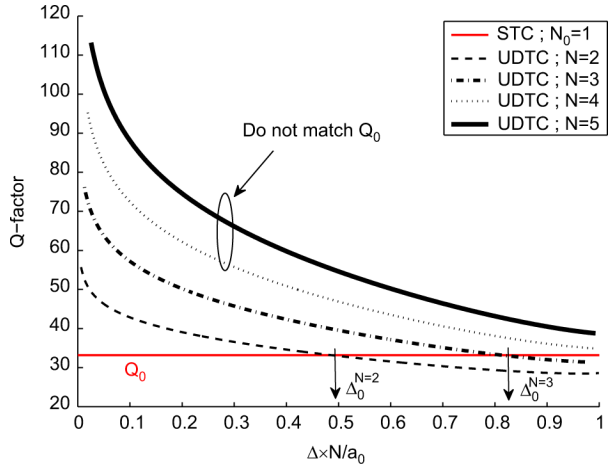

Fig. 3. Variation of Q-factor as a function of $\Delta \times N/a_0$; $D = 0.05$ m.

Earlier, the authors in [19] have reported an antenna using equal spacing Δ between two adjacent turns, so the i^{th} turn radius is given by $a_i = a_0 - (i-1)\Delta$; using equal Δ, a UDTC antenna is presented in Fig. 2(b). It will be shown that the UDTC provides an improved H with an unconstrained Q over the STC; this only occurs when $2 \leq N \leq 3$ and designs with $N > 3$ are nevertheless limited by fabrication.

For the demonstration, the responses of the resulting antennas are predicted, the UDTCs are compared to the STC and the preliminary results presented in Fig. 3. For the comparison, the variation of Q for certain $N = 2$ to 5 UDTC designs with uniform Δ spacing is used. The respective Q-factors for each of the corresponding coils are calculated using (10) and (11) in (1) and with the following assumptions: $D = 0.05$ m, the section of the wire $S_{wire} = 0.05$ mm^2, and $a_0 = 0.07$ m($a_0 = \sqrt{2}D$, [26]). Results, Fig. 3, indicate that at low Δ, the Q is higher for each of the UDTC designs than for the STC (represented by Q_0). Although, for $N \leq 3$, Q can be decreased to match Q_0 (at optimum $\Delta_0^{N=2}$ and $\Delta_0^{N=3}$), for $N \geq 4$, Q does not match Q_0 and therefore an unconstrained Q solution is no longer possible. Note that, contradictorily, designs having $N = 2$ can not be designated as UDTCs since they are only made of two turns and hence of a single Δ.

Concluding, the UDTC antenna of Fig. 2(a) overcomes the STC design, Fig. 2(a), and showed, Fig. 3, a non-compromised Q-factor for $N = 2$ and 3. Earlier reported, N is related to H and only $N = 2$ and $N = 3$ can play a part. This is perceived as a limitation for the UDTC design since a higher N can not be accomplished. Furthermore, the uniform spacing Δ does not allow for maximum exploitation of the turns and to enhance H a non-uniform spacing is proposed. We hereby present a derived coil antenna design whose internal turns can be rearranged and successfully exploited towards a higher H. Subsequently, this novel antenna is termed non-uniformly distributed-turns coil

(NDTC) and presented next. The final NDTC design will be shown to have advantage of maximum possible enhanced H with unconstrained Q.

III. Proposed Non-Uniformly Distributed-Turns Coil Design

In this section, the design of an NDTC antenna is presented. As with the UDTC, the NDTC antenna, shown in Fig. 2(c), is made of N number of turns given by a radius vector $\mathbf{A} = [a_1, a_2, \ldots a_N]$, and a constant current I. To optimally design the NDTC antenna, we assume a predefined Tag at a distance D. The optimization is performed by maximizing the H of the antenna while maintaining the Q-factor of the proposed antenna unconstrained. The necessary analytical formulation for the optimization is presented next and subsequently detailed.

1) H Formulation: The total expected H-field for a typical multi-turn coil antenna (e.g., DTC) at a distance D from the center of the coil is given by the sum of the H-fields produced by each of the N turns [12], and is expressed as

$$H(\mathbf{A}) = \sum_{i=1}^{N} \frac{I \cdot a_i^2}{2\left[\sqrt{a_i^2 + D^2}\right]^3}. \tag{7}$$

2) Q Formulation: The Q-factor of the NDTC antenna is hereby introduced as Q_1, and is obtained from (1) using L_1 and R_1, the inductance and the resistance of the NDTC antenna, respectively. The inductance L_1 of a multi-turn coil antenna (e.g., NDTC) with N turns is obtained as the sum of the self-inductances of individual turns and the mutual inductances between them [20]. For a single turn of radius a, the self-inductance, L, is calculated as

$$L(a, S_{wire}) = \mu_0 a \left(\ln\left(\frac{8\sqrt{\pi}a}{\sqrt{S_{wire}}} - 2\right)\right) \tag{8}$$

where S_{wire} is the section of the wire. And, the mutual inductance, M, between two turns having radius a_i and a_j is calculated as

$$M(a_i, a_j) = \mu_0 \sqrt{a_i a_j}\left[\left(\frac{2}{\kappa} - \kappa\right)K(\kappa) - \frac{2}{\kappa}E(\kappa)\right] \tag{9}$$

where $\kappa = 2\sqrt{a_i a_j}/(a_i + a_j)$, and $K(\kappa)$ and $E(\kappa)$ are the complete elliptic integrals of the 1^{st} and 2^{nd} kind respectively [20]. Hence, using (8) and (9), L_1 is given by

$$L_1(\mathbf{A}) = \sum_{i=1}^{N} L(a_i, r) + \sum_{i=1}^{N}\sum_{j=1}^{N} M(a_i, a_j)(1 - \phi_{ij}), \tag{10}$$

where ϕ_{ij} is one for $i = j$ and zero otherwise. The resistance R_1 of the multi-turn coil antenna depends mainly on the conductor length (the total length of the turns) and an approximate value is given by [23] as

$$R_1(\mathbf{A}) = \frac{1}{\sigma \cdot S_{wire}} \sum_{i=1}^{N} 2\pi a_i \tag{11}$$

where $\sigma = 5.9 \times 10^7/\Omega m$ is the conductivity of copper. We notice that, $L_1(\mathbf{A})$ and $R_1(\mathbf{A})$ in (10) and (11), respectively, are functions of $\mathbf{A}$. Therefore, substituting L_1 and R_1 in (1), provides Q_1 which is a function of $\mathbf{A}$ (thereby, Q_1 and $Q_1(\mathbf{A})$ are used interchangeably).

A. Optimization Formulation

In this Section, the necessary formulation for the optimization of the NDTC antenna design is presented. In Section II-B.1, the optimum radius of the coil antennas presented in Fig. 2, was given as $a_0 = \sqrt{2}D$. In the case of NDTC, the radius of each turn, a_i, that encompasses the antenna design must satisfy $0 < a_i \leq \sqrt{2}D$. For fare comparisons, the current I of the NDTC antenna is equal to that of the STC (I_0). For the optimization of the NDTC, we find an optimum radius, a_i, for every turn a_1 to a_n (optimum vector $\mathbf{A}$) that maximizes H with unconstrained Q-factor ($Q_1 = Q_0$ for this purpose). The analytical design procedure is proposed subsequently and the optimization problem (finds best solution) is formulated as

$$\begin{aligned} \underset{\mathbf{A}}{\text{maximize}} \quad & H(\mathbf{A}) \\ \text{subject to} \quad & Q_1(\mathbf{A}) = Q_0 \\ & 0 < a_i \leq \sqrt{2}D \end{aligned} \tag{12}$$

where $H(\mathbf{A})$ is given by (7) and $Q_1(\mathbf{A})$ is obtained by substituting (1) by $L_1(\mathbf{A})$(10) and $R_1(\mathbf{A})$(11) and fully expressed as

$$Q_1(\mathbf{A}) = \omega \frac{\sum_{i=1}^{N} L(a_i, r) + \sum_{i=1}^{N}\sum_{j=1}^{N} M(a_i, a_j)(1 - \phi_{ij})}{\frac{1}{\sigma \cdot S_{wire}} \sum_{i=1}^{N} 2\pi a_i}. \tag{13}$$

The Lagrangian, $\mathcal{L}$, of the optimization problem (12) can be written as

$$\mathcal{L}(\lambda, \mathbf{A}) = H(\mathbf{A}) + \lambda\left(Q_1(\mathbf{A}) - Q_0\right) \tag{14}$$

where λ is the $\mathcal{L}$ multiplier. Subsequently, for the H maximization, the partial differential equations and related partial derivatives of $\mathcal{L}$ (w. r. t. a_i and λ) are equated to zero

$$\begin{aligned} \frac{\partial \mathcal{L}}{\partial a_i} = 0 &\Longrightarrow \frac{\partial}{\partial a_i} H(\mathbf{A}) + \lambda \frac{\partial}{\partial a_i} Q_1(\mathbf{A}) \\ &= 0; \quad i \in [1, N], \\ \frac{\partial \mathcal{L}}{\partial \lambda} = 0 &\Longrightarrow Q_1(\mathbf{A}) = Q_0 \end{aligned} \tag{15}$$

where, the N variables ($a_i = a_1$ to a_N) of the optimum radius vector $\mathbf{A}$ can be obtained and satisfy the $N + 1$ non linear equations. Because unfortunately, (15) evolves complex nonlinear equations, as a consequence, a close form analytical solution is hard to obtain. We therefore propose the following computational algorithm, for the solution, next.

Algorithm for the Optimum $\mathbf{A}$

A computational algorithm for the fine solution of (12) is hereby proposed and presented in Table I. In essence, it initializes with $a_i = \sqrt{2}D, \forall\, i \in [1, N]$, and $0 < a_i \leq \sqrt{2}D$. In each iteration, the turn radii is decreased by a step size δ (we assumed a minimum possible separation, g, between adjacent turns due to fabrication limits), and H and Q_1 are computed iteratively until $Q_1 = Q_0$ and H is maximized; this will result in a final

TABLE I
COMPUTATIONAL ALGORITHM FOR OPTIMUM $\mathbf{A}$

```
Initialization:
I ⇐ I_0
a_i ⇐ √2D (in mm), ∀ i ∈ [1, N]
δ ⇐ 0.1
g ⇐ 0.45
B ⇐ A
Iteration:
while(B(1) > 0)
   B(2) ⇐ B(1) − g
   while(B(2) > 0)
      B(3) ⇐ B(2) − g
      while(B(3) > 0)
         .
         .
         .
         B(N) ⇐ B(N − 1) − g
         Q_1 = 0
         while(B(N) > 0)
            Calculate Q_1 and H for set B using (7) and (13)
            if (Q_1 is equal Q_0)
               Get A(optimum) ⇐ B with Maximum H
            end
            B(N) ⇐ B(N) − δ
         end
         .
         .
         .
      end
      B(2) ⇐ B(2) − δ
   end
   B(1) ⇐ B(1) − δ
end
```

coil which has distributed turns arranged computationally for the highest H possible and unconstrained Q.

TABLE II
ANALYTICAL RESULTS OF H-FIELD ENHANCEMENT FOR OPTIMAL NDTC ANTENNA DESIGNS

Design	Q-factor	H (A/m)	$\frac{(H-H_0)}{H_0}\%$
STC	33.165	1.500	0
NDTC $N=2$	33.162	2.587	72.47
NDTC $N=3$	33.162	3.017	101.13
NDTC $N=4$	33.164	3.207	113.80
NDTC $N=5$	33.164	3.275	118.33
UDTC $N=2$	33.163	2.587	72.47
UDTC $N=3$	33.164	2.9755	98.37
UDTC $N \geq 4$	n/a	n/a	n/a

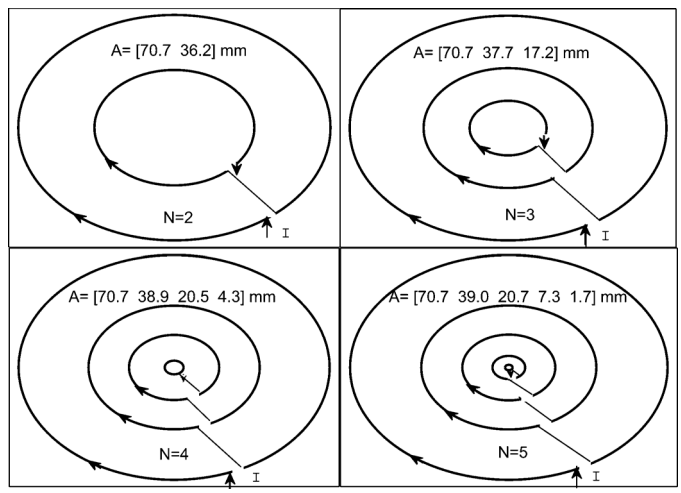

Fig. 4. Optimal NDTC antennas for various N; $D = 0.05$ m; $S_{wire} = 0.05$ mm^2; $I_0 = 0.4$ A.

IV. RESULTS

The proposed Algorithm and the presented formulation-study is now validated. For the validation, we compare the results of the STC and the NDTC antennas obtained analytically with those from an Electromagnetic Solver commonly used for Antenna modeling and analysis. In addition, we provide analytical results comparison between the UDTC and the NDTC antennas to claim the latter as the leading design.

A. Analytical Results

The analytical study was carried out using MATLAB; other mathematics-based simulators can be used. The following criteria for the development of the NDTC antenna compared to the STC: $D = 0.05$ m, $S_{wire} = 0.05$ mm^2, $a_0 = 0.07$ m ($a_0 = \sqrt{2}D$, [26]), $N_0 = 1$ and $H_0 = H_{min} = 1.5$ A/m (rms value specified in ISO-14443 [4]) led to $I_0 = 0.4$ A using (6). Initial results are given in Table II which shows an STC antenna of $Q_0 = 33.165$; this value is sufficient for reliable data transfer [23]. The related H of the STC antenna is also provided.

We now use the algorithm of Table I to find optimum $\mathbf{A}$ for various values of N in the NDTC design. The respective responses are given in Table II and the final prototypes showing their computed radius vector $\mathbf{A} = [a_1, a_2, \ldots a_N]$ presented in Fig. 4. Table II shows how the final NDTC designs achieve an improved H and unconstrained Q as compared to the STC design. The STC antenna ($H = 1.5$ A/m and $N_0 = 1$) is provided for the comparison purpose. In essence, a significant enhancement of 72.47% (in the H-field) for just one turn increment, $N = 2$, is reported in Table II and this enhancement is shown to increase for higher values of N. Results for the UDTC design are also included. When the UDTC and the NDTC designs both are $N = 2$, present identical H performance; this is because with only two turns the radiating elements distribution is identical in both designs. For $N = 3$ in both the designs, the NDTC presents a small but significant 2.76% over the UDTC. Because designs having $N \geq 4$ are not viable in UDTCs (Q becomes compromised and different than Q_0, Fig. 3) and NDTC is realizable for $N = 5$, the final comparison between these two designs favors the NDTC in a 19.96% H increase over UDTC.

The latest optimized NDTC design having $N = 5$ reports the highest H value of 118.33% improvement over the STC and a significant 19.96% over the UDTC. NDTC designs having $N > 5$ are unfortunately not realizable due to manufacturing surface-plane limitations for an element projected inside the area of $N = 5$ (the inner element), Fig. 4. Thereby, we propose $N = 5$ as the best solution for the proposed NDTC antenna design. Concluding remarks from results indicate that the theoretical analysis presented, positively contributes to a significantly enhanced H antenna design without compromising the Q-factor; by smartly exploiting the unused (internal) area of a coil antenna.

TABLE III
SIMULATED RESULTS OF H-FIELD ENHANCEMENT FOR OPTIMAL NDTC ANTENNA DESIGNS

Design	Q-factor	H (A/m)	$\frac{(H-H_0)}{H_0}\%$	C1 (pF)	C2 (pF)
STC	31.33	1.491	0	173.80	40.56
NDTC $N=2$	31.35	2.521	69.08	97.64	31.28
NDTC $N=3$	31.27	2.920	95.84	78.07	28.43
NDTC $N=4$	31.18	3.109	108.52	70.59	27.27
NDTC $N=5$	31.16	3.224	116.23	67.73	26.81

B. Simulated Results

Simulated results are now presented. Using commercially available software Zeland IE3D, based on the Method of Moments (MoM), the H-field of the immediately earlier introduced antenna coils are compared over the STC. For the simulation we use $a_1 = 70.7\ \mathrm{mm}$ and strip width 0.25 mm and strip height 0.2 mm (hence, $S_{wire} = 0.05\ \mathrm{mm}^2$). Results are presented in Table III and reports a NDTC design of $N = 2$ having a 69.08% higher H compared to the STC; once again, the STC antenna is provided for comparison purposes. Earlier reported in Section IV-A the H enhancement increases for higher values of N to one extend where designs having $N > 5$ are not realizable. The latest optimized NDTC design having $N = 5$, reports the highest H value of 116.23% improvement over the STC. Concluding simulations (not provided for brevity) indicated that higher values of $N = 5$ were irrelevant for the improvement of H due to fabrication limits. By observation, the results of Table III show fair agreement to those achieved mathematically in Table II. Thus, validating the Analysis-study presented in this paper for the delivering of bespoke coil antennas. The difference is accredited to fabrication; the simulated coils are planar.

In addition, using IE3D, the corresponding values of the lumped capacitors $C1$ and $C2$ required for the excitation, Fig. 1, of the reported antennas, Fig. 2, are given in Table III; this allowed the antennas resonating at 13.56 MHz. Future work is proposed using fabricated prototypes with commercially available, cost-effective integrated capacitors $C1$ and $C2$ and measured results to perceive dissimilarities.

V. CONCLUSION

An NDTC antenna for an enhanced H-field in HF-RFID applications has been presented. For the H-field improvement, the number of turns of the radiating element encompassing the antenna, were increased and arranged optimally with novel favored non-uniform separation (unequal spacing between the turns). To validate the new design, a fair comparison was made to a reference design (STC) having comparable Q-factor. The proposed NDTC design had unconstrained Q-factor achieved by optimally arranging and adjusting the number and spacing between the turns, such that the H-field was maximized. The results were validated mathematically and by simulation and showed a tailored NDTC design with an improved H-field and unconstrained Q-factor compared to a reference STC antenna design. The new NDTC design claims a 116.23% higher H compared to the STC and a significant 19.96% over the UDTC. The fair agreement between the simulated and the mathematically-based results validates the Analysis-study presented in this paper.

REFERENCES

[1] C. A. Balanis, *Antenna Theory Analysis and Design*, 2nd ed. New York, NY, USA: Wiley, 1997.

[2] Y. Lee, Antenna Circuit Design for RFID Applications Microchip Technology Inc, 2003 [Online]. Available: http://ww1.microchip.com/downloads/en/appnotes/00710c.pdf

[3] Z. Tang, Y. He, Z. Hou, B. Li, and Z. Tang, "The effects of antenna properties on read distance in passive backscatter RFID systems," in *Proc. Int. Conf. Networks Security, Wireless Commun. Trusted Comput.*, Wuhan, China, Apr. 2009, pp. 120–123.

[4] *Identification Cards-Contactless Integrated Circuit(s) Cards-Proximity Cards-Part 3: Initialization and Anticollision, Int. Std. ISO/IEC 14443–3*, ISO/IEC/JTC1 Inf. Technol Std 1999 [Online]. Available: http://www.waazaa.org/download/fcd-14443-3.pdf

[5] B. Jiang, J. R. Smith, M. Philipose, S. Roy, K. Sundara-Rajan, and A. V. Mamishev, "Energy scavenging for inductively coupled passive RFID systems," *IEEE Trans. Instrum. Meas.*, vol. 56, no. 1, pp. 118–125, Feb. 2007.

[6] N.-G. Choi, H.-J. Lee, and S.-H. Lee, "A 13.56 MHz RFID system," in *Proc. Asia-Pacific Conf. Appl. Electromagnetics (APACE)*, Johar, Malaysia, Dec. 2005, pp. 289–292.

[7] L. Qiwei, "Research and design on radio frequency identification reader," in *Proc. IEEE Int. Workshop Anti-Counterfeiting, Security, Identification*, Xiamen, China, Apr. 2007, pp. 356–359.

[8] J. Kim, H. Kim, J. Kim, J. Cho, G. Kim, and S. Kim, "13.56 MHz RFID reader SiP with embedded antenna," in *Proc. Elect. Design Advanced Packaging Syst. Symp. (EDAPS)*, Seoul, South Korea, Dec. 2008, pp. 186–189.

[9] Y.-C. Choi, M.-W. Seo, Y.-H. Kim, and H.-J. Yoo, "Multi-standard 13.56 MHz RFID reader system," in *Proc. 23rd Int. Technical Conf. Circuits/Syst., Comput. Comm.*, Yamaguchi, Japan, Jul. 2008, pp. 1073–1076.

[10] A. Goulbourne, *HF Antenna Design Notes*, Texas Instruments Inc, Sep. 2003 [Online]. Available: http://www.ti.com/rfid/docs/manuals/appNotes/HFAntennaDesignNotes

[11] S. S. Basat, L. Kyutae, J. Laskar, and M. M. Tentzeris, "Design and modeling of embedded 13.56 MHz RFID antennas," in *Proc. Antennas Propag. Society Int. Symp.*, Washington, DC, Jul. 2005, vol. 4B, pp. 64–67.

[12] K. Fotopoulou and B. W. Flynn, "Optimum antenna coil structure for inductive powering of passive RFID tags," in *Proc. IEEE Int. Conf. RFID*, Grapevine, TX, USA, Mar. 2007, pp. 71–77.

[13] F. Ohnimus, I. Ndip, S. Guttowski, and H. Reichi, "Design and analysis of a bent antenna-coil for a HF-RFID transponder," in *Proc. 38th Eur. Microw. Conf.*, Amsterdam, Netherlands, Oct. 2008, pp. 75–78.

[14] U.-M. Jow and M. Ghovanloo, "Design and optimization of printed spiral coils for efficient transcutaneous inductive power transmission," *IEEE Trans. Biomed. Circuits Syst.*, vol. 1, no. 3, pp. 193–202, Sep. 2007.

[15] N. Rueangsri and A. Thanachayanont, "Coil design for optimum operating range of magnetically coupled RFID system," in *Proc. Int. Symp. Comm. Info. Tech.*, 2006, pp. 1199–1202.

[16] D. Wang, L. Xu, H. Huang, and D. Sun, "Optimization of tag antenna for RFID system," in *Proc. Int. Conf. Info. Technol. Comput. Sci.*, Kiev, Ukraine, Jul. 2009, pp. 36–39.

[17] S. Salleh, K. Salleh, M. F. Hashim, and Z. A. Majid, "Design and analysis of 13.56 MHz RFID antenna based on modified Wheeler equation: A practical approach," in *Proc. Int. Conf. Electronic Devices, Syst. Appl.*, Kuala Lumpur, Malaysia, Apr. 2010, pp. 326–330.

[18] W. Aerts, E. D. Mulder, B. Preneel, G. A. E. Vandenbosch, and I. Verbauwhede, "Dependence of RFID reader antenna design on read out distance," *IEEE Trans. Antennas Propag.*, vol. 56, no. 12, pp. 3829–3837, Dec. 2008.

[19] A. Sharma, I. J. G. Zuazola, A. Gupta, A. Perallos, and J. C. Batchelor, "Enhanced H-field in HF-RFID systems by optimizing the loop spacing of antenna coils," *Microw. Opt. Technol. Lett.*, vol. 55, no. 4, pp. 944–948, Apr. 2013.

[20] C. M. Zierhofer and E. S. Hochmair, "Geometric approach for coupling enhancement of magnetically coupled coils," *IEEE Trans. Biomed. Eng.*, vol. 43, no. 7, pp. 708–714, Jul. 1996.

[21] X. Chen, W. G. Yeoh, Y. B. Choi, H. Li, and R. Singh, "A 2.45-GHz near-field RFID system with passive on-chip antenna tags," *IEEE Trans. Microw. Theory Tech.*, vol. 56, no. 6, pp. 1397–1404, Jun. 2008.

[22] J. Nummela, L. Ukkonen, L. Sydnheimo, and M. Kivikoski, "13,56 MHz RFID antenna for cell phone integrated reader," in *Proc. IEEE Antennas and Propagation Soc. Int. Symp.*, Hawaii, USA, Jun. 2007, pp. 1088–1091.

[23] C. Reinhold, P. Scholz, W. John, and U. Hilleringmann, "Efficient antenna design of inductive coupled RFID-systems with high power demand," *J. Commun.*, vol. 2, no. 6, pp. 14–23, Nov. 2007.
[24] X. Qing and Z. N. Chen, "Characteristics of a metal-backed loop antenna and its application to a high-frequency RFID smart shelf," *IEEE Antennas Propag. Mag.*, vol. 51, no. 2, pp. 26–38, Apr. 2009.
[25] C. Bowick, *RF Circuit Design*. Burlington, MA, USA: , 1997.
[26] K. Finkenzeller, *RFID Handbook*, 2nd ed. New York, NY, USA: Wiley, 2003.
[27] D. Staelin, A. Morgenthaler, and J. Kong, *Electromagnetic Waves*. Englewood Cliffs, NJ, USA: Prentice-Hall, 1994.

Ashwani Sharma received the B.Tech. degree from LNM IIT, Jaipur, India, in 2010 and the M.S. degree in technology and communication systems from ETSIT, Technical University of Madrid (UPM), Madrid, Spain, in 2013. He is currently pursuing the Ph.D. degree at the University of Deusto, Bilbao, Spain.

His research works are published in various international journals and conferences such as IEEE Letters, IET journals, and Wiley letters. His current research interests include antenna design and integration, single and multi band antennas.

Ignacio J. Garcia Zuazola (M'11) received the B.Eng. (with honors) in telecommunications engineering from Queen Mary—University of London (2003), the HND in telecommunications engineering from the college of North West London (2000), the FPII in industrial electronics from the School of Chemistry and Electronics of Indautxu, Spain (1995), and the Ph.D. degree in electronics (microwaves, antennas) part-time program in 2008 and his viva in 2010.

He was employed as a Research Associate (2004) University of Kent, Canterbury, U.K., Research Engineer, to senior position Grade 9/9, (2006) University of Wales, Swansea, U.K. and Research Associate (2008) University of Kent, Canterbury, U.K. He holds educational awards in Electrical wiring, Pneumatic and Hydraulic systems, and Robotics. He was hired by industry for Babcok & Wilcox (1993), Iberdrola (1995), Thyssen Elevators (1998), and Cell Communications (2000), and self-engaged in a SME in electrical wiring (1996). He is currently (2011) a Senior Research Fellow in Microwaves Engineering (Antennas) at the University of Deusto, Bilbao, Spain and a current Visiting Senior Research Fellow at the I3S, University of Leeds, UK. His current research interests include single-band and multiband miniature antennas, and the use of Electromagnetic-Band Gap (EBG) structures and Frequency-Selective Surfaces (FSS).

Anshu Gupta received the B.Tech. degree from LNM IIT, Jaipur, India. He is currently pursuing the Ph.D. degree at Helmut Schmidt University, Hamburg, Germany.

He has authored and coauthored 35 papers in the field of antenna and radar processing in international journal and conferences. His current research interests include antenna design and integration, radar signal processing, software defined radar, over the horizon radar.

Mr. Gupta received the Best Paper Award at International Radar Symposium 2012. He serves on the review board of *IET Radar Sonar and Navigation*.

Asier Perallos received the B.Sc. degree in computer engineering, the M.Sc. degree in software engineering and the Ph.D. degree from the University of Deusto, Biscay, Spain.

He has over 10 years of experience as a Lecturer in the Computer Engineering Department, Faculty of Engineering , University of Deusto. His academic background has been focused on teaching in software engineering, distributed systems and web quality evaluation. He is the Director of Master's in Development and Integration of Software Solutions at the University of Deusto and is the Principal Researcher of DeustoTech Mobility research team in Deusto Foundation. He has more than a decade of experience developing and managing R&D projects, with dozens of projects and technology transfer actions led.

John C. Batchelor (S'93–M'95–SM'07) received the B.Sc. and Ph.D. degrees from the University of Kent, Canterbury, U.K., in 1991 and 1995, respectively.

From 1994 to 1996, he was a Research Assistant with the Electronics Department, University of Kent, and in 1997, became a Lecturer of electronic engineering. He now leads the Antennas Group at Kent and is a Reader in Antenna Technology. His current research interests include UHF RFID tag design, body-centric antennas, printed antennas, compact multiband antennas, electromagnetic bandgap.